Supplement of Atmos. Chem. Phys., 26, 11235–11253, 2026
https://doi.org/10.5194/acp-26-11235-2026-supplement

Atmospheric Chemistry and Physics
Open Access

Supplement of

Fractal characteristics of ice-supersaturated regions in the tropopause region of the northern midlatitudes

Helena Zoe Schuh et al.

Correspondence to: Helena Zoe Schuh (hschuh01@students.uni-mainz.de)

S1 Justification the use of area-perimeter relation

As observed by Cheng (1995), the "dimension" D as derived by the area-perimeter relation does not agree with the Hausdorff dimension in general. This raises the question if the use of this relation and thus the obtained value D is meaningful at all. Nevertheless, this method is frequently employed to ascertain fractal dimensions and analyze the respective objects. Already Mandelbrot et al. (1984) found that the dimension D obtained by area-perimeter relations agrees with fractal dimensions obtained by spectral analysis. Sakellariou et al. (1991) also discussed this issue, and concluded that the method is "the most stable and least ambiguous method" for obtaining fractal dimensions. In Klinkenberg (1994) other methods for determining fractal dimensions are reviewed. While the dimension D calculated using the area-perimeter relation $P = C \cdot A^{\frac{D}{2}}$ does not satisfy the mathematical definition of the fractal dimension, it is appropriate to use this approach in order to study the fractal characteristics and properties of phenomena. As these naturally occurring phenomena are not perfect fractals, a pragmatic approach such as the area-perimeter relation is sufficient for a relevant evaluation. Finally, Florio et al. (2019) showed that for island-type objects, such as our ISSRs, the area-perimeter approach is meaningful and results into dimensions close to the classical fractal dimensions.

S2 Changes due to coarsening of the grid

For a rigorous definition of fractal dimensions (in the Hausdorff sense) one would have to send the grid resolution to zero, i.e. approaching an infinitely small length scale for measuring perimeters and areas, respectively. Only in the limit, the fractal dimensions are well defined. We cannot obtain this limit, as we are limited by the highest resolution of the ERA5 data, which is $0.25° \times 0.25°$ on an isobar surface. Instead, we can check the robustness of the fractal properties by artificial coarsening of the data and redoing the evaluation in terms of calculating the fractal dimension for the coarser objects. For this purpose, we introduced two different data sets, i.e. a **coarse** set (half resolution, i.e. $0.5° \times 0.5°$), and a **very coarse** set (quarter resolution, i.e. $1° \times 1°$). In both cases, we use the same ERA5 data, i.e. a full set of 11 years (2010-2020).

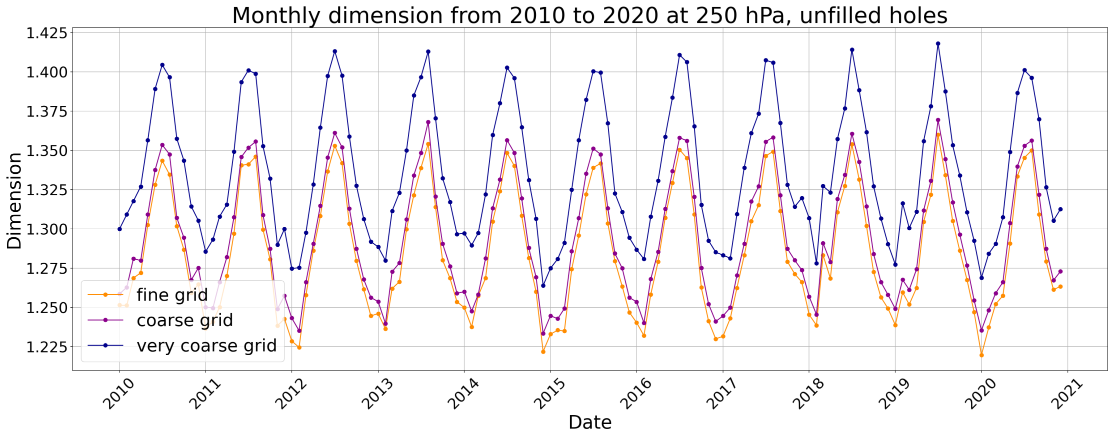

Figure S1: Fractal dimensions at pressure level $p = 250\,\text{hPa}$ for different grid resolutions (fine $0.25° \times 0.25°$ in orange, coarse $0.5° \times 0.5°$ in violet, and very coarse $1° \times 1°$ in dark blue) in a monthly resolution for the time span of 11 years of ERA5 data.

In Figure S1 we exemplarily show the results for the pressure level $p = 250\,\text{hPa}$; for the other two pressure levels we find qualitatively the same features (not shown). For all grid resolution we still find the signature of self-similarity, i.e. a fractal dimension of $D > 1$.

There is a similar qualitative change if we proceed from coarser to finer grid resolution. The highest values of D are found for the very coarse resolution, with a jump in order of $\Delta D \sim 0.04 - 0.06$ to the coarse resolution. The next step to the fine (i.e. ERA5 native) resolution is then much smaller, the difference is in order of $\Delta D \sim 0.01 - 0.02$. More precisely, the dimension seems to qualitatively "converge" to the values of the fine resolution, based on 3 available grid resolutions. For the other pressure levels, we find the same behavior, and comparable values of the difference in D.

Thus, we can conclude that the fractal properties seem to be robust over all tested grid resolutions. Surprisingly, the highest values of the fractal dimension can be obtained for the coarsest resolution of $1^\circ \times 1^\circ$, whereas the self-similarity is still prominent for the ERA5 resolution. Finally, we can state that the behavior is exactly the same for the filled versions of ISSR, as described in the following section S3.

We find that for coarse grids the fractal dimension is higher than for high resolution. This is indeed counter-intuitive, but there is a satisfactory explanation. Comparing the total area (summed up per month) across resolutions, we observe the area staying roughly the same. This makes sense as both some supersaturated and some subsaturated pixels will be lost in the process of lowering the resolution. Comparing the total perimeter (summed up per month) across resolutions, we can see the perimeter being smallest for the lowest resolution. This is expected as we smooth out edges. A constant area and lower perimeter should intuitively lead to a lower fractal dimension. Here, we need to remember that the dimension for a single month is not calculated with the sums of area and perimeter, but as a regression slope with the individual areas and perimeters of single ISSRs. Looking at the average perimeter per ISSR, we see a significantly higher ratio for the very coarse resolution. This is caused by the coarsening "melting" ISSRs together that were previously separated by thin subsaturated gaps. Thus, a higher perimeter per ISSR raises the dimension.

S3 Fractal dimension - additional evaluations

S3.1 Additional plots for the summer season

Here we present the determination of the fractal dimension for three pressure levels in case of July 2020.

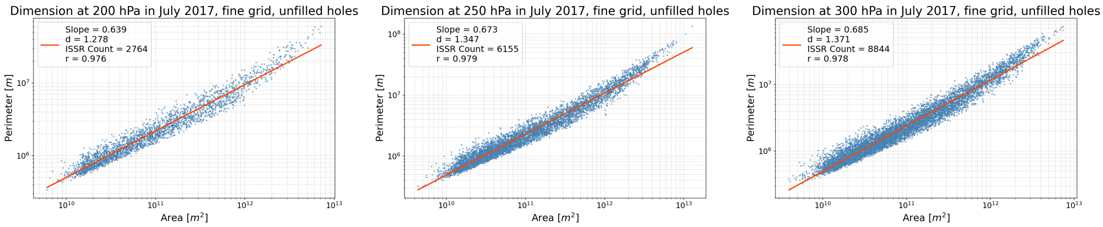

Figure S2: Determination of the fractal dimension via fits to the area-perimeter relation in case of July 2017. Blue dots indicate the data points (A,P), red lines are the fits from linear regression. Left: Pressure level $p = 200\,\text{hPa}$; Middle: Pressure level $p = 250\,\text{hPa}$; Right: Pressure level $p = 300\,\text{hPa}$

S3.2 Changes due to filled objects

In our investigations so far, we used the derived islands of ISSRs as we found them. Thus, these regions can have holes, as can be seen clearly in Figures 3 and 4 of the manuscript. These holes increase the perimeter of the objects in our calculations, changing the fractal dimension, as discussed by Brinkhoff et al. (2015). This aspect can be seen from two different point of views.

1. We are investigating objects with an assumed self-similarity. As a consequence of this assumption we would expect the same structural properties on every scale, i.e. repeating the main features when we zoom into smaller scales. As known from theory there are objects like e.g. the Sierpinski triangle or the Sierpinski carpet (e.g., Florio et al., 2019) with holes, leading to the general structure of the object, and also to the respective fractal dimension. For clouds as macroscopic objects on different scales, we might assume a similar property. If we zoom into a smaller scale, we still find some holes in the cloudy object, thus we could assume that the "holes" inside the ISSRs should be an important feature. A similar feature can be seen in case of high resolution measurements of water vapor, leading to pathlengths of ISSRs on a much smaller scale (see discussion in Spichtinger and Leschner, 2016, their section 5). From this point of view, the use of unfilled ISSRs would be meaningful, or even mandatory, since their structure with holes is a key feature of the objects.

2. Following the discussion by Brinkhoff et al. (2015), holes in the observed objects (clouds, ISSRs, etc.) might artificially result from the detection procedure. Since it is not really clear which features are real and which are of artificial nature, it is more meaningful to fill the holes and to evaluate the filled objects. This procedure was suggested by Brinkhoff et al. (2015) and was also applied by Christensen and Driver (2021).

These two aspects are relevant for our further investigation. So far, we have used the first approach, using the ISSRs as they are, assuming that the holes are relevant for the inherent structure of these objects. To investigate the impact of a possible erroneous description of islands, we repeat the evaluation of the whole data set using a filling of occurring holes in the islands rather that eliminating the objects with holes.

In Figure S3 we show the results of the monthly timeseries of fractal dimension on the three pressure levels. We find that the qualitative behavior of the monthly derived

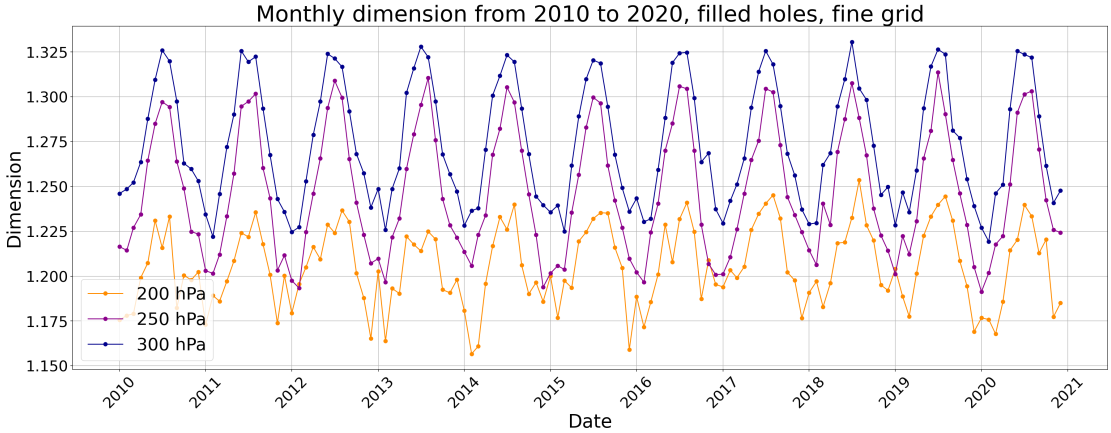

Figure S3: Fractal dimensions at three pressure levels (200 hPa in orange, 250 hPa in violet, and 300 hPa in dark blue) in a monthly resolution for the time span of 11 years of ERA5 data; the possibly occurring holes in the ISSRs islands are filled.

fractal dimension remains the same, even for the filled ISSRs. We still see the vertical layering of the dimension at different pressure levels with the same seasonal cycle as the unfilled ISSRs.
There is, as expected, a change in the values of the fractal dimensions. The values of D for filled objects are reduced by an absolute value of about $\Delta D \sim 0.03 - 0.05$, with smallest deviations for the pressure level $p = 200\,\text{hPa}$ and largest deviations for the pressure level $p = 300\,\text{hPa}$. Nonetheless, the filled objects show the feature of a self-similarity with dimensions $D > 1$.

S3.3 Results using filled holes

In this section, we present the corresponding figures based on the data set with filled holes. These results complement the analysis shown in the main text, where primarily the unfilled-hole data were discussed.

The purpose of including the filled-hole data is to demonstrate the robustness of the identified statistical characteristics of ISSR horizontal extents with respect to the treatment of internal gaps. While minor quantitative differences may occur, the overall behavior of the distributions, including their seasonal dependence and characteristic regimes, remains consistent. The following figures therefore provide a direct comparison to the results presented in Section 4 of the manuscript.

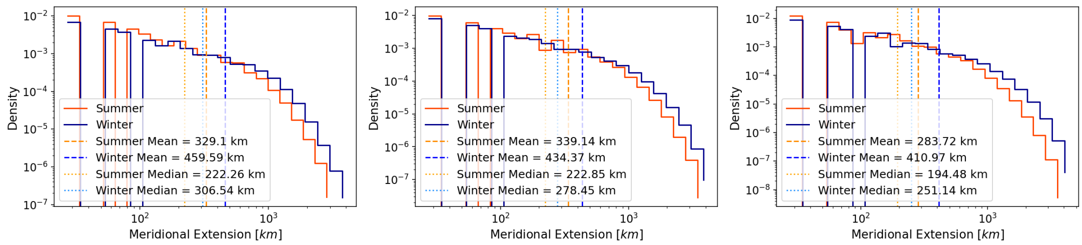

Figure S4: Distributions of meridional span (i.e. pathlengths in North-South direction) for different seasons, i.e. summer (JJA, orange colors) and winter (DJF, blue colors) using data with filled holes. Mean values are indicated by vertical dashed lines, median values are indicated by vertical dotted lines. Left: 200 hPa, Middle: 250 hPa, Right: 300 hPa

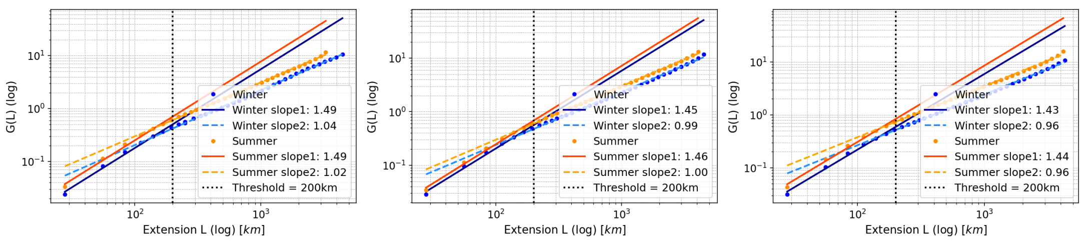

Figure S5: Weibull plots for the pathlength distributions in North-South direction using data with filled holes. The linear regression fit is shown for the regimes of pathlengths smaller and larger than $\sim 2 \cdot 10^2$km, this threshold being indicated by a dotted line. Blue/orange colors indicate winter/summer data, respectively. The fits to the different regimes are represented by a dashed and a solid line. Left: 200 hPa, Middle: 250 hPa, Right: 300 hPa

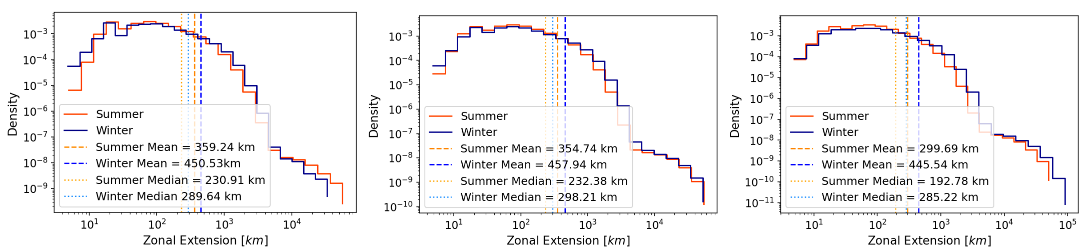

Figure S6: Distributions of zonal span (i.e. pathlengths in East-West direction) for different seasons, i.e. summer (JJA, orange colors) and winter (DJF, blue colors) using data with filled holes. Mean values are indicated by vertical dashed lines, median values are indicated by vertical dotted lines. Left: 200 hPa, Middle: 250 hPa, Right: 300 hPa

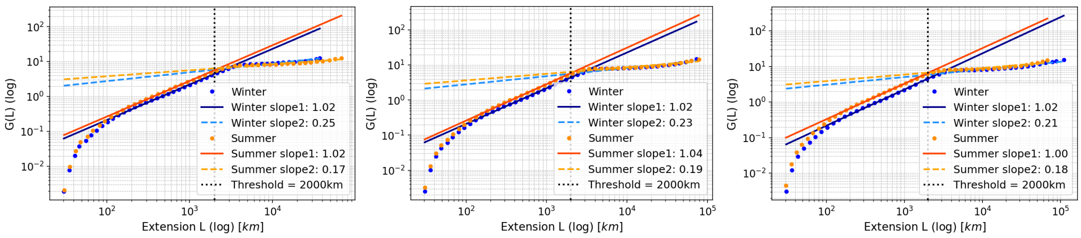

Figure S7: Weibull plots for the pathlength distributions in East-West direction using data with filled holes. The linear regression fit is shown for the regimes of pathlengths smaller and larger than $\sim 2 \cdot 10^3$km, this threshold being indicated by a dotted line. Blue/orange colors indicate winter/summer data, respectively. The fits to the different regimes are represented by a dashed and a solid line. Left: 200 hPa, Middle: 250 hPa, Right: 300 hPa